

# Morphometry of volcanic cones on Mars in perspective of Astrobiological Research

Michael Gilichinsky<sup>1</sup>, Nikita Demidov<sup>2,3</sup> and Elizaveta Rivkina<sup>2</sup>

<sup>1</sup>Department of Forest Resource Management, Swedish University of Agricultural Sciences, Umeå, Sweden. Affiliation at the time of manuscript preparation

<sup>2</sup>Institute of Physicochemical and Biological Problems in Soil Science, Russian Academy of Sciences, Pushchino 142290, Russia  
e-mail: [elizaveta.rivkina@gmail.com](mailto:elizaveta.rivkina@gmail.com)

<sup>3</sup>Vernadsky Institute of Geochemistry and Analytical Chemistry, Russian Academy of Sciences, Moscow 119991, Russia

**Abstract:** The permanently frozen volcanic sediment is one of the most promising geological objects for searching life on Mars. On Earth, volcanic intrusions into permafrost result in formation of the unique microbial communities. We propose several terrestrial analogues of Martian polar volcanoes, such as the permanently frozen volcanic sediments on the Kamchatka peninsula and in Antarctica. The present study shows applicability of the morphometric analysis for demonstration of the morphological similarity between the terrestrial and Martian cinder cones. In the present work, the morphometric analysis of young Martian landforms is based on the assumption that the conical structures identified on digital terrain model (DTM) are volcanic cinder cones. Morphometric analysis of the studied cones showed a range of degradation. The extent of degradation may be an indicator of age based on comparison with volcanic cinder cones on Earth. A morphometric analysis of potentially young volcanic cones in the North Polar Region of Mars was performed to estimate their relative age. The 14 potential cinder cones were identified using the DTM provided by Mars Express High Resolution Stereo Camera (HRSC), allowing for the basic morphometric calculations. The majority of the cinder cones are localized in the Chasma Boreale region within the area 79°–81°N and 261°–295°E. The calculated morphometric parameters showed that the cone average steepness varied from 3.4° to 11.8°, cone height-to-width ratio varied from 0.025 to 0.12, and the ratio between surface and basal area of the cone varied from 1.005 to 1.131. The studied cinder cones were classified with respect to the morphometric ratios assuming that larger values correspond to the younger structures. Employing the terrestrial analogy of morphometric ratios as a proxy for relative geological age, we suggest that existing microorganisms may be found in permafrost of young Martian cinder cones.

Received 6 March 2015, accepted 16 April 2015, first published online 29 May 2015

**Key words:** cinder cones, DTM, HRSC, Mars, morphometry, volcanic permafrost

## Introduction

The studies of extra-terrestrial volcanoes were largely promoted in preparation for NASA lunar missions in late 1960s and early 1970s (Nemeth 2011). Mars had a long history of volcanic activity which resulted in presence of large number of volcanic landforms (Carr 2006). Martian volcanism is different from that on Earth due to its lower gravity, lower atmospheric pressure and the lack of plate tectonics. Crater statistics of calderas of several Tharsis volcanoes based on Mars Express High Resolution Stereo Camera (HRSC) imagery reveals ages of ~100 Ma (Neukum *et al.* 2004). Crater size–frequency for lower flanks of Olympus Mons suggests age as young as 2.5 Ma. Cerberus plains also contain some of the youngest volcanic features on the planet of not more than a few million years old (Berman & Hartmann 2002). Several shield volcanoes concentrated at the North Polar cap margin based on the data of Mars Global Surveyor's instrument Mars Orbiter Laser Altimeter (MOLA) were dated from 1 to 20 Ma (Garvin *et al.* 2000).

In the Chasma Boreale region, 106 mounds were identified and analysed based on the MOLA topographic data in

combination with high-resolution imagery from the Thermal Emission Imaging System (THEMIS) instrument on board of the Mars Odyssey spacecraft, Mars Orbiter Camera (MOC) and High-Resolution Imaging Science Experiment (HiRISE) camera on board of the Mars Reconnaissance Orbiter (Warner & Farmer 2008). It was suggested that the part of mounds located in this region are erosional remnants and not volcanic landforms. However, the North Polar deposits are the youngest geological units on Mars (Fishbaugh & Head 2002). Among the North Polar morphological features observed with HRSC imagery was a field of small cones, near the mouth of Chasma Boreale (Neukum & van Gasselt 2006). These cones were identified using digital terrain model (DTM) in combination with HRSC high-resolution colour images. The surrounding dark deposits and the absence of erosion features lead to suggestion that these landforms are potentially recent cinder cones. The absolute age of these structures has been estimated as 7–15 Myr (Herkenhoff & Plaut 2000).

Within the ongoing discussion about geological nature of the polar cones, the biological implication of cinder cones in Mars is very important. Theoretically, the presence of life is possible in sub-permafrost aquifers which may be transported through

volcano to the surface. On Earth, this process was studied in Kamchatka, where thermophilic microorganisms were extracted from the permafrost volcanic deposits surrounding cinder cones (Abramov *et al.* 2008). Terrestrial, non-volcanic permafrost deposits ranging in age up to 8 Ma exist in the Arctic and Antarctic and contain viable microorganisms (Gilichinsky *et al.* 2007; Gilichinsky & Rivkina 2011).

#### *Origin of volcanic cinder cones*

Terrestrial cinder cones are 'perhaps the simplest and most common volcanic landforms in existence' (Wood 1980). It is a monogenetic volcanic structure with a distinct and defined initial date of formation that lasts not more than a few million years, before erosional processes flatten it. Morphological and morphometric methods have proven to be an efficient tool for determining the relative dates of terrestrial cinder cones and the erosional processes affecting them (Wood 1980; Hasenaka & Carmichael 1985; Hooper 1995; Inbar & Risso 2001; Parrot 2007). Such analysis generally attempts to measure the morphometric parameters of cinder cones, e.g. height, diameter, and slope, and the relationship between them. Modern morphology of cinder cones might be associated with the duration of the denudation processes.

On Earth, there are large volcanic fields with hundreds of monogenetic cinder cones, such as the Michoacan–Guanajuato (Mexico), San Francisco (Arizona, USA), Andino–Cuyano (Mendoza, Argentina), Tenerife (Canary Islands, Spain) and Hawaii with a long list of published works (Scott & Trask 1971; Porter 1972; Bloomfield 1975; Settle 1979; Martin del Pozzo 1982; Dohrenwend *et al.* 1986; Wolfe *et al.* 1987; Hooper 1995; Inbar & Risso 2001; Dóniz *et al.* 2008).

The variation in the morphometric parameters of the cinder cones within the same climate zone might be associated with the relative morphometric dating with the more recent cinder cones characterized by steeper slopes. However, the comparison of cinder cones of similar age from different climatic zones shows that the erosional rates directly affect their geometrical attributes and provide a range of morphometric parameters. The intensive erosional processes in the climatic conditions of the Kamchatka peninsula are not allowing for preservation of cinder cones older than 100 Ky (Gilichinsky & Rivkina 2011; Inbar *et al.* 2011). The cones dated as Early–Middle Pleistocene age were eroded due to the geomorphic processes, particularly during the last stage of the Pleistocene glaciation. On the contrary, the subtropical climate of the Mexican Volcanic field (Hooper 1995), the semiarid climate of Payun Matru Volcanic Field (Inbar & Risso 2001) or the Mediterranean climate of the Golan plateau (Inbar *et al.* 2008) are showing measurable morphological changes in the range of hundred thousands of years. Recent monogenetic cinder cones formed in the Great Fissure Tolbachik Eruption (Kamchatka, Russia) or Parícutin (Mexico) have steep slopes, up to 30°, although older eroded scoria cones typically have gentler slopes, from 10° to 15° (Golan plateau, Israel). The influence of climate is reflected in the highest rates of erosion in the area, due to the harsh weather conditions. The slope

angle decreases from the initial value of 31°–34° for the 1975 cones to 25°–29° for the cones 1500–2000 years before present (BP). The Parícutin cone in Mexico erupted in the year 1943 had the initial slope of ~33° (Seegerstrom, 1950) declining slightly to 31°, 45 years later (Inbar *et al.* 1994). Recent cones on Mt Etna show a slope decrease of 10° in only 450 years (Wood 1980).

Based on the theoretical considerations, Martian cinder cones will resemble those on Earth in general shape but might be larger in size and lower in height, due to Mars lower gravity and atmospheric pressure (Wilson & Head 1994; Fagents & Wilson 1996; Parfitt & Wilson 2008; Broz *et al.* 2014). Previous predictions (Wilson & Head 1994, Mouginitis-Mark *et al.* 1992) suggested that even mild Strombolian eruptions such as those that construct steep-sided (23°–33°) scoria/cinder cones on Earth would result in broad 5–10 km diameter cones under Martian conditions, with typical flank slopes of ~10°. However, Wood (1979) assumed that cinder cone steepness is independent of gravity and atmospheric pressure, because the wider dispersal of ejecta material would affect crater width and basal diameter in the same way.

#### *Martian cinder cones*

While large volcanoes on Mars have been long studied in detail, smaller mounds were not considered as an object of study due to the absence of high resolution imagery. The recent release of the high resolution data made possible the precise analysis of Martian surface terrain. In modern studies, several fields of conical mounds were analysed suggesting various hypotheses about their origin as volcanic (Neukum & Gasselt 2006), erosional remnants (Warner & Farmer 2008), mud volcanoes (Pondrelli *et al.* 2011), pingos (de Pablo & Kamatsu, 2009) and of impact craters (Hodges & Moore 1994). Such cones were not studied yet by rovers and the origin of majority of conical structures is still disputed.

In the early reports from the HRSC team seven volcanic cones were observed in the Martian North Pole Region (Neukum & van Gasselt 2006; Broz & Hauber 2012). These cones may have been formed from the cinder material that surfaced as a result of the underground volcanic activity. Although the study suggested that cinder cones may have erupted within a few tens of thousands years, the cones appearing in the imagery are remarkably unaffected by erosion from wind, water, or ice moving in the soil. The analysis of 106 mounds in the same region showed cones slope ranging between 1° and 8° and cones width between 3 and 18 km. In spite of some similarity with terrestrial basaltic low-angle volcanoes, this field of cones was interpreted as being remnants of near-polar layered material (Warner & Farmer 2008). The basis for this consideration was horizontal flank layering, polygonal map-view morphology, topographic relationships and spatial association with retreating polar scarps. The cinder cones of the Martian North Polar Region are localized in the area within 79°–81°N and 261°–295°E. The age of the shield volcanoes in the same area was estimated at 1–20 Ma (Garvin *et al.* 2000).

Mars Reconnaissance Orbiter's Context Camera (CTX) imagery was used to analyse volcanic field in south-west Utopia

Planitia (Lanz *et al.* 2010). The results showed similarities to volcanic rift zones on Earth: a set of broad eruptive fissures, parallel dike swarms, magmatic intrusions and number of lava flows that can be seen to have erupted from the fissures and cones (Lanz *et al.* 2010). Cones superposed on the fissures are interpreted to be volcanic cinder cones based on the similarity with other features rather than morphometry.

The data from several cameras such as CTX, HRSC and HiRISE were used for analysis of Tharsis region (Broz & Hauber 2012). Twenty-nine volcanic cones were identified and their morphometric parameters were calculated using basal width, crater width, height and slope. Slopes of Tharsis cinder cones were estimated to vary from 13° to 28°, with basal width as much as 1–4 km. The results suggested that the studied cones are Martian equivalents of terrestrial cinder cones. The age estimations of cinder cones were based on the crater size–frequency distribution of surrounding surfaces suggesting formation between 1.5 and 0.44 Ga.

#### *Microbiological potential of Martian volcanic permafrost*

The cinder cones are the only known so far geological formations on Mars that might be relevant to the permafrost life preservation model. The presence of thermophilic microorganisms in the frozen terrestrial volcanic sediments raises questions about their source. High-temperature ecological niches in the areas of active terrestrial volcanism are known as geothermal oases among permanently frozen ash and scoria (Cousins & Crawford 2011; Flores *et al.* 2013; Herbold *et al.* 2014). The only way for thermophiles to be present within frozen pyroclastic material is through deposition during the eruption. Such terrestrial microbial community might serve as a model for extraterrestrial inhabitants on Earth-like cryogenic planet Mars with its numerous ancient extinct volcanoes. Their past eruptions were periodically breaking out the planet's cryosphere by magma fluxes, forming the thermal oases. The products of eruptions are lifted to the surface and frozen. These newly frozen volcanic deposits are much younger than surrounding permafrost. The cap at the Martian North Pole is formed by water ice and provides the environment for microbial life preservation. At the early Noachian time 4.6–3.7 billion years ago, Mars was evolving in a similar scenario with the early Earth, which could support the appearance of life.

At Hesperian (3.7–1.8 billion years ago) and Amazonian time (1.8 billion years ago–present), the global freezing took place on Mars. In the post-Noachian time, geothermal oases could be formed on the frozen surface. Those oases have been associated with volcanic activity and located in ground water effusion areas where microorganisms could penetrate from below. However, due to the great difference in the age of permafrost it is difficult to extend experience of terrestrial cryobiosphere to its Martian analogues.

The most promising location for the search of life signs is permanently frozen sediments of the polar volcanoes. These regions include several young cinder cones and shield-volcanoes at the edge of polar ice cap. There are several Earth analogues of Martian polar volcanoes such as permanently frozen volcanic sediments at Kamchatka peninsula and Antarctic

volcanoes. Thus, terrestrial permafrost may represent a possible ecosystem for Mars as an Earth-like cryogenic planet.

In the present work, the morphometric analysis of young Martian landforms is based on the assumption that the conical structures identified within digital terrain model are volcanic cinder cones. Assuming the volcanic origin of the conical structures in the Martian North Polar Region, we applied the morphometric method to estimate their relative age. By employing the terrestrial analogy of morphometric ratios as a proxy for geological age, we suggest that microorganisms are likely to be found in permafrost of Martian cinder cones.

## Methodology

### *HRSC DTM data*

The data from Mars Express HRSC image archive at the Freie Universitaet ([hrscview.fu-berlin.de](http://hrscview.fu-berlin.de), Berlin, Germany) were used for description of the volcanic terrain. The HRSC experiment on the Mars Express Mission provides high-resolution surface imagery, accompanied by elevation data. The HRSC data are delivered at different processing levels, including radiometric calibration, geometric corrections, spatial referencing and DTM derivation. The archived HRSC Level-4 products (colour images and DTM) allow for the detail investigation of morphometric parameters of smaller topographic features such as possible cinder cones. The elevation in HRSC DTM is calculated relative to the MOLA equipotential surface (areoid) and directly comparable with MOLA topography values.

The image data of HRSC are organized in north–south oriented strips of various length and 52 km wide swath, captured at resolution of  $\sim 50$  m pixel<sup>-1</sup> in the colour mode. The resolution of corresponding DTM varies between 50 and 250 m pixel<sup>-1</sup>. However, the DTM coverage largely depends on the quality of stereo images and is not necessarily produced for the entire portion of the image data.

The 14 high-resolution colour Level-4 images accompanied by HRSC-based DTM of the North Polar Region were acquired from the Mars Express HRSC image archive for two groups of cinder cones. Although the larger number of low-level HRSC images is available for the region, the study area was restricted to the DTM coverage (Fig. 1).

### *Survey of cinder cones*

In our study, the survey of cinder cones was performed using the HRSC optical data in combination with corresponding DTM. In total, 35 conical structures from 25 imaging orbits (i.e. image covers, according to the HRSC experiment nomenclature) were studied. The main prerequisite for the visual survey was the definition of a cinder cone. Within the available DTM cover there are a lot of features that may provide the formal definition of a cinder cone as conical volcanic structure. However, the combination of high-resolution optical data with DTM has allowed for more specific description of cinder cones:

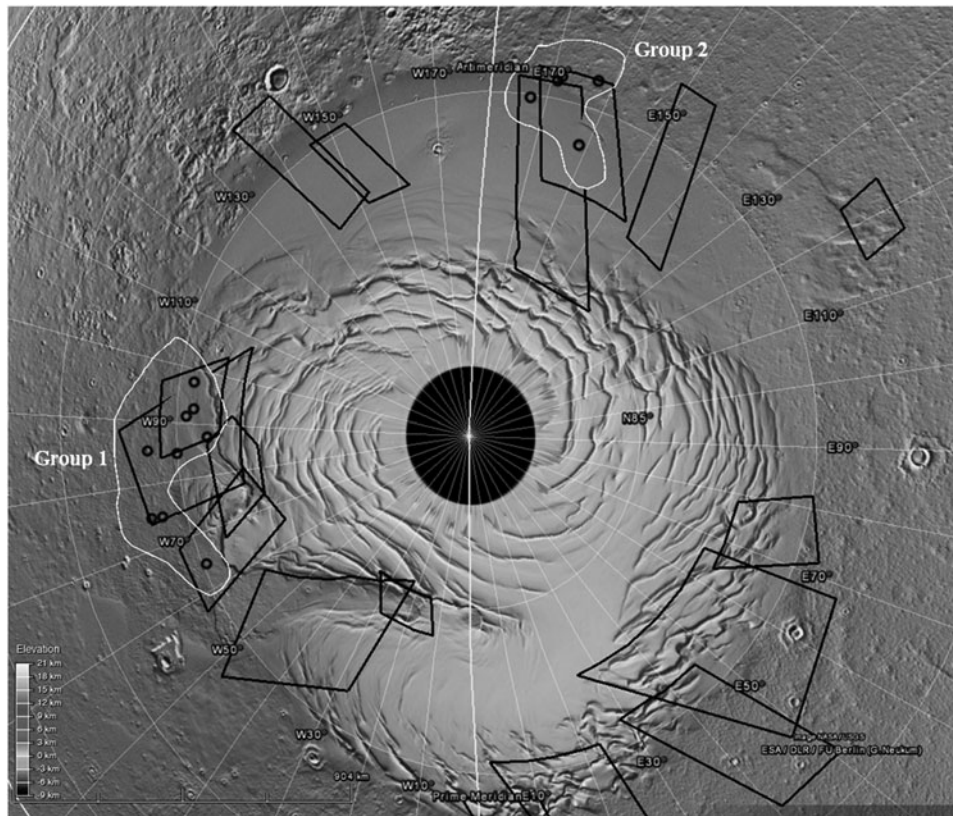


**Fig. 1.** Grey-shaded terrain of the Martian North Polar Region extracted from Google Mars ([google.com/mars](http://google.com/mars)) showing the available HRSC Level-4 DTM cover (black polygons) and two studied groups of cinder cones (white polygons). The Martian North Circumpolar Area is marked as a black circle.

- Symmetrical conical structures distinguishable from the topographic surrounding in DTM;
- Straight flanks and evident summit craters with respect to relatively small size of the entire mound;
- Noticeable in the HRSC colour scene and different enough to merit a visual separation from the image background.

Only 14 cinder cones (within five orbits) met the aforementioned conditions (Table 1). It should be noted that beyond the DTM coverage, we found additional 15 conical structures that could be associated with volcanic activity.

#### *Morphometric analysis*

We conducted morphometric measurements of the Martian conical structures using the method previously tested on Kamchatka cinder cones (Gilichinsky & Rivkina 2011). All conical features deemed similar to those of the terrestrial cinder cones were identified and their morphometric parameters were calculated from the available HRSC DTM coverage.

The central point for the estimation of morphometric parameters is the delineation of the basal isoline that separates the cinder cone from the surrounding topographic background. We have calculated the slope models of the identified cinder cones as an elevation change parameter in the DTM, using the topographic modelling module in Exelis ENVI/IDL. Using the calculated slope model, the basal isoline was

allocated according to the cinder cone lowest elevation isoline with the average slope of more than 5°. The definition of the base has allowed for calculation of the morphometric parameters as ratios of the cone geometrical attributes (Fig. 2).

The ratio between the surface area ( $S_a$ ) and the planimetric area of the cone base ( $S_b$ ) provides a direct indication of cinder cone roughness (surface-to-base ratio). In a grid-based system such as HRSC DTM, planimetric area is calculated as a sum of areas of individual cells, which is defined by the DTM spatial resolution. The surface area of each grid cell is dependent on its slope. A surface area increases as a grid cell is tilted from a horizontal reference plane to its three-dimensional (3D) position in a DTM (Fig. 2). The surface area of individual cell ( $S'_a$ ) can be calculated by dividing the planimetric area by the cosine of corresponding slope angle ( $\alpha$ ). Then the total surface area of the cone is calculated as sum of the individual cells (equation (1)).

$$S_a = \sum \frac{S'_a}{\cos(\alpha)} \quad (1)$$

Computation of the surface (lateral) area of a cinder cone will result in a value that is greater or equal to the area of the rectangle on the planimetric reference grid of DTM. For example, in case of ideal cone with  $S_b = 1 \text{ km}^2$  and slope of 30°, the ratio will be equal to 1.15. Removal of the cone material by erosion will smoothen the topography resulting in the ratio decrease overtime.

Table 1. Morphometric parameters of 14 cinder cones as measured from HRSC DTM

Cone ID	HRSC orbit	Location	Volume (km <sup>3</sup> )	Height, <i>m</i>	Average slope (°)	Base area ( <i>S<sub>b</sub></i> ) (km <sup>2</sup> )	Surface area ( <i>S<sub>a</sub></i> ) (km <sup>2</sup> )	Basal width ( <i>W<sub>b</sub></i> ) (km)
1	1275_0000 <sup>1</sup>	80.23N, 295.68E	3.11	593	11.8	17.4	19.6	2.3
2	3737_0000 <sup>1</sup>	81.26N, 272.42E	4.42	455	10.1	14.4	15.7	2.1
3	3737_0000 <sup>1</sup>	80.73N, 267.26E	3.23	316	6.4	19.7	20.3	2.5
4	3737_0000 <sup>1</sup>	80.65N, 262.29E	3.37	387	6.9	16.3	16.9	2.3
5	3737_0000 <sup>1</sup>	80.46N, 268.74E	2.69	153	3.5	25.4	25.6	2.8
6	1169_0000 <sup>2</sup>	78.69N, 285.33E	10.96	557	7.9	47.2	49.5	3.9
7	1169_0000 <sup>2</sup>	80.08N, 275.33E	2.32	255	3.4	33.7	34.0	3.3
8	1169_0000 <sup>2</sup>	78.91N, 274.65E	6.03	240	4.7	26.5	27.0	2.9
9	1169_0000 <sup>2</sup>	79.14N, 285.52E	2.21	257	6.1	16.1	16.5	2.3
10	1291_0000 <sup>3</sup>	80.13N, 172.45E	2.29	198	3.2	29.6	29.9	3.1
11	1258_0000 <sup>4</sup>	81.15N, 161.13E	3.17	180	3.3	34.2	34.5	3.3
12	1258_0000 <sup>4</sup>	79.36N, 168.08E	1.35	170	5.4	11.4	11.6	1.9
13	1258_0000 <sup>4</sup>	79.51N, 168.62E	3.19	177	1.8	46.1	46.2	3.8
14	1258_0000 <sup>4</sup>	79.21N, 162.25E	0.59	101	2.3	12.1	12.2	1.9

Note that superscript numeration of HRSC orbits is referring to the spatial resolution of a corresponding DTM as follows: 1–150, 2–250, 3–100 and 4–125 m. Locations of the cinder cones are given in planetocentric coordinates.

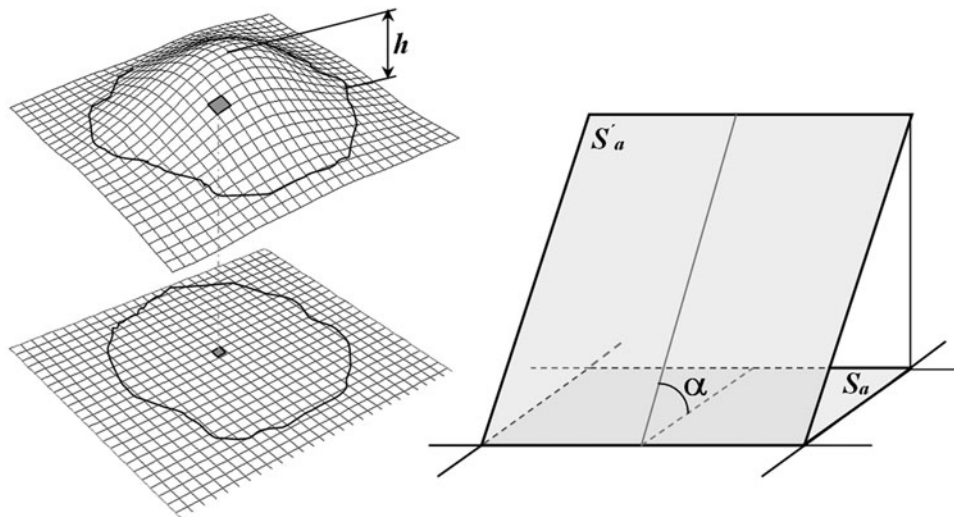


**Fig. 2.** Volcanic cone as represented by DTM and by planimetric grid (a). The height of the cone (denoted as *h*) is defined as elevation difference between the highest cone point and the basal isoline; Example of relation between planimetric reference grid and the corresponding cell of the tilted plane (b). The surface area is denoted as *S'<sub>a</sub>*, planimetric area as *S<sub>a</sub>* and the slope angle as  $\alpha$ .

The standard morphometric measure of the overall steepness of a cinder cone is calculated as ratio of the height (*h*) to the basal width (*W<sub>b</sub>*). The height is calculated as a difference between the crest elevation and the elevation of the base of the cone. The basal width is calculated as  $\sqrt{S_b/\pi}$ .

Similarly to *S<sub>a</sub>/S<sub>b</sub>* ratio, this ratio also reflects the erosion of the cone and decreases with age as material is removed from the crest to the base. Originated from the traditional morphometric measurements from topographic maps, the *h/W<sub>b</sub>* (height-to-width ratio) has to be supported by DTM derived *S<sub>a</sub>/S<sub>b</sub>* ratio.

The volume of the cinder cones is calculated using the surface of cinder cones with respect to a reference plane. Similarly to all the aforementioned morphometric parameters, the calculation of volume is an approximation, largely depending on the DTM spatial resolution. We have calculated the

volume of the inferred cinder cones according to equation (2):

$$V = \sum h' S'_b \quad (2)$$

where *h'* is the elevation difference in an individual grid cell between the surface elevation and the elevation of the base of the cone and *S'<sub>b</sub>* is the cone base area in an individual grid cell.

The factor of DTM spatial resolution is very important for estimation of morphometric parameters. The HRSC DTM provides the description of Martian topography in resolutions varying from 50 m at the equator to 250 m at the poles. Thus, the reduced resolution of DTM available for the study of 100–150 m in the North Pole region allows for the correct estimation of basic morphometric parameters mentioned above but not necessarily sufficient for calculation of summit and crater attributes.

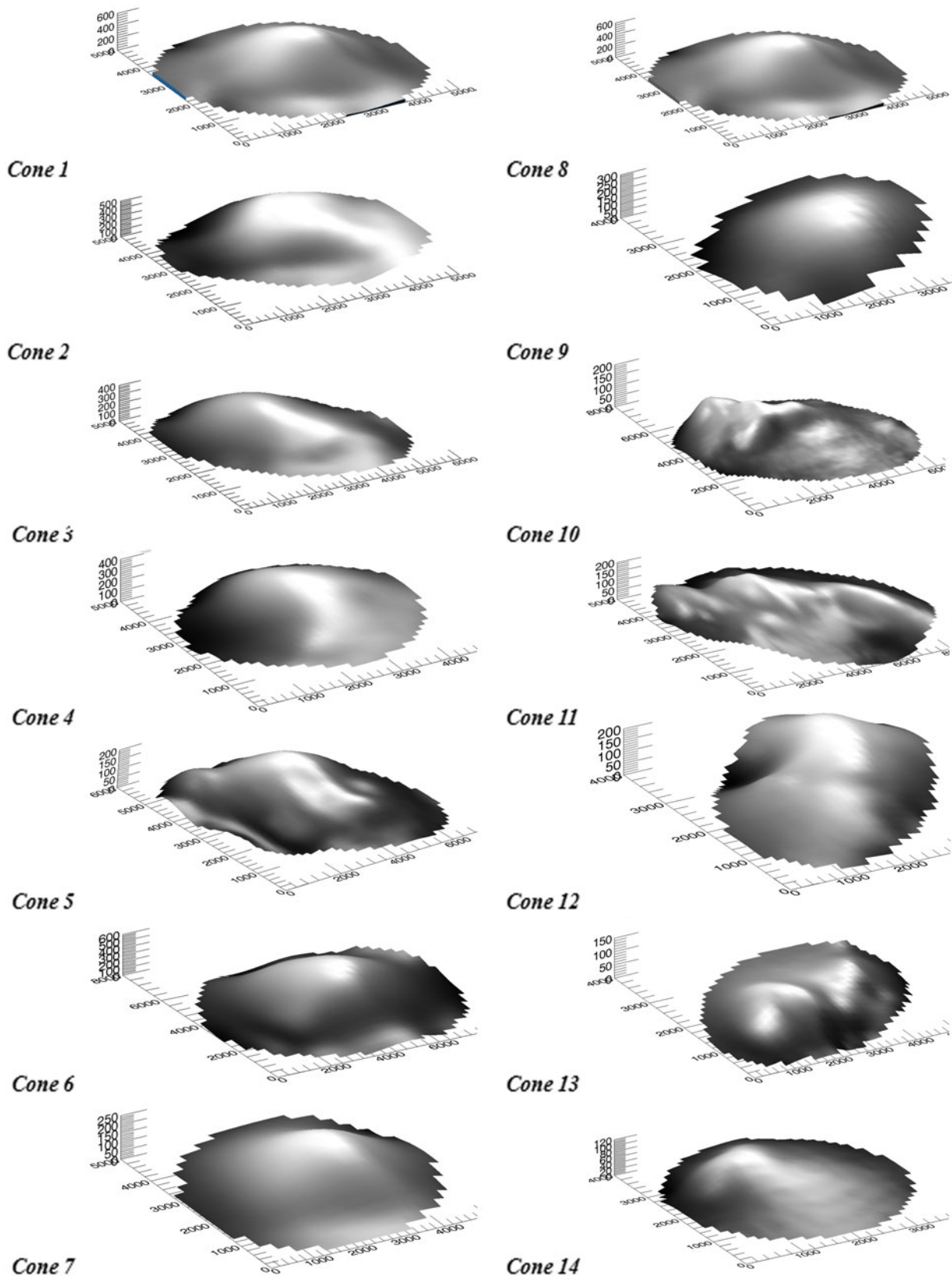


**Fig. 3.** The digital terrain models of the 14 studied cinder cones. The numeration of the cones conforms the order in Table 1. Note that the cones 1–9 belong to the Chasma Boreale group (Group 1) and cones 10–14 belong to the Olympia Udinae group (Group 2).

## Results

Fourteen cones divided into two geographic groups were observed in the Martian North Polar Region. They are covered by 25 HRSC orbits for which DTM Level 4 exists (Fig. 1). The spatial resolution of the studied DTM varied between 100 and 250 m, the height of the cones varied in the range from 250 to 600 m (Table 1).

The first group (Group 1) centred on 80°N; 270°E (approximately 300 km west of the mouth of Chasma Boreale) and the second group (Group 2) is located to the west of Olympia Undae dune field (80°N; 165°E). All these cones were identified in the landscape by visual examination and the DTM for each cone was extracted from the general orbit coverage. This allowed for visualization of main morphological attributes as flank slopes, summit units and basal outlines (Fig. 3).

For each cone, calculations were made of the main morphological parameters such as height, width, average slope, volume, basal and surface areas (Table 1).

Group 1 consists of nine conical mounds with the average slope of 6.8° and the average surface-to-base ratio of 1.05 (Cones 1–9, Table 1). The calculated volume of the cones in the group varied between 2.21 and 10.96 km<sup>3</sup> with the average volume of 4.26 km<sup>3</sup>. Group 2 consists of five cones with the average slope of 3.2° and the average surface-to-base ratio of 1.01 (Cones 10–14, Table 1). The calculated volume of the cones in the group varied between 0.59 and 3.19 km<sup>3</sup> with the average volume of 2.12 km<sup>3</sup>.

Calculations were based on cone plane attributes in case of height-to-width ratio and cone 3D characteristics in case of surface-to-base ratio. The height-to-width and surface-to-base ratios are usually consistent with the erosion-based scoria wasting process of the material from the top of cinder cone to its flanks. The association between these parameters allows for straightforward degradation modelling of local topography by interpolation of DTM data points. The height-to-width and surface-to-base ratios show a common shift from larger values within Group 1 towards smaller values in Group 2 (Fig. 4). The variation of height-to-width ratio ranges between 0.04 and 0.14 in cones of Group 1 and between 0.025 and 0.04 in cones of Group 2. Similarly, the variation in surface-to-base ratio ranges between 1.01 and 1.14 (Group 1) and between 1.002 and 1.017 (Group 2). The comparison with four recent terrestrial cinder cones visualizes the correspondence between these two types of morphometric ratios. However, it should be noted that the strictly numerical comparison of these parameters with terrestrial analogues is not applicable due to incomparable DTM resolution.

The per-cone average slope values were calculated and compared with  $S_a/S_b$  values demonstrating good correlation,  $R^2 = 0.901$  (Fig. 5). Similarly to terrestrial analogues, this relationship associates ‘recent’ cones with steeper slopes as having greater surface area, in comparison with cone’s base. Similarly, ‘older’ cones are associated with gentle average slopes and having surface area almost equal to cone’s base.

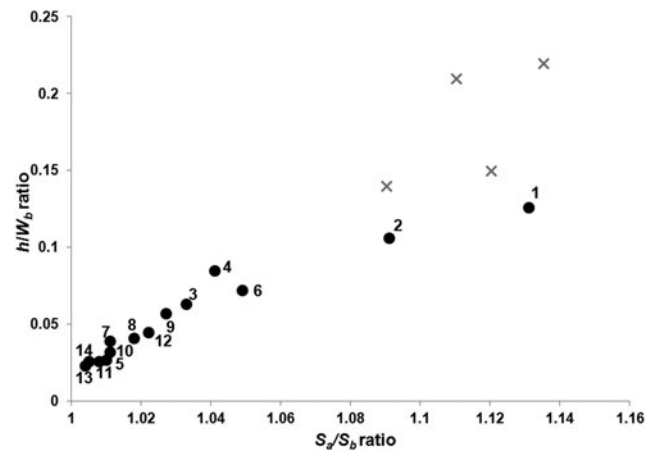


**Fig. 4.** Comparison of planimetric height-to-width ratio ( $h/W_b$ ) against terrain surface-to-base ratio ( $S_a/S_b$ ) as calculated from HRSC DTM. The numeration of the cones conforms the order in Table 1. Note the four recent terrestrial cinder cones (marked as grey crosses) that were formed in Great Fissure Tolbachik Eruption in Kamchatka between years 1975 and 1976.

## Discussion

In previous studies, it has been shown that Earth volcanic permafrost contains viable thermophilic microorganisms (Abramov *et al.* 2008; Gilichinsky *et al.* 2010a, 2010b; Mironov *et al.* 2013). These types of microorganisms were never found in permafrost located outside the volcanic areas. The only way they are to appear within a frozen material is through a concurrent deposition during the eruption, together with products associated with volcano heated subsurface geothermal oases. Thus, in the areas of active volcanism, the catastrophic geological events transport the life from the depths of the high-temperature ecological niches out to the surface where it may be preserved in permafrost over a long period of time.

Following Earth analogy, life may survive in Martian permafrost up to 8 Myr. For this reason, the focus of our study is the North Polar Region of Mars. Although the Martian South Polar Region shows indications of water ice as well, the putative young volcanic structures were not observed there. The Martian North Polar Region satisfies two main astrobiological requirements: the presence of ice-cemented ground (permafrost) and relatively young volcanic structures as cinder cones. In this case, a classification of cinder cones by morphometric parameters might be used for relative dating assuming younger structures as having a higher astrobiological potential from the life conservation perspective.

The results obtained in our study provide an additional aspect of Mars habitability by considering morphometric ratios as a proxy for relative geological age. The nine cones of the Group 1 range (Cones 1–9, Table 1) were previously identified by Neukum *et al.* (2004) and Neukum & van Gasselt (2006) as conical mounds of volcanic origin. In the present study, the slopes of this group were found to have a smaller range than that of 16°–28° reported by Broz & Hauber (2012) for Tharsis pyroclastic cones. Their findings are similar to the

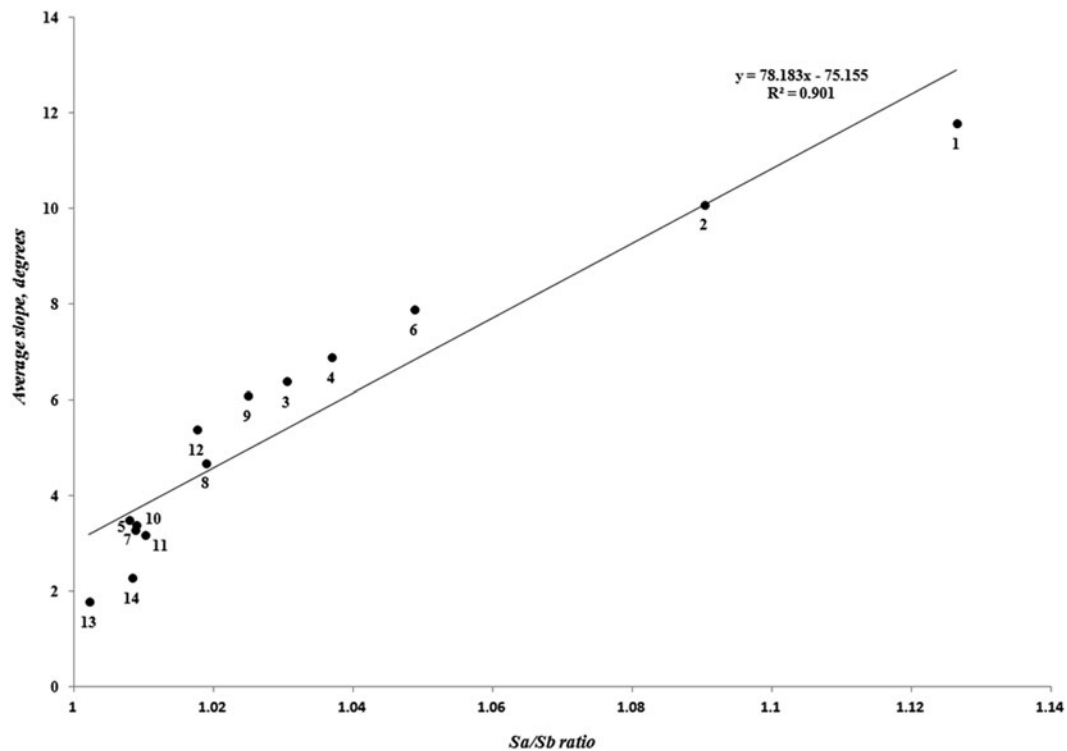


**Fig. 5.** Comparison of per-cone average slope mapped against values of  $S_a/S_b$  ratio, calculated from the HRSC DTM. The numeration of the cones conforms the order in Table 1.

range measured for young terrestrial cinder cones in Kamchatka (Gilichinsky & Rivkina 2011) and Payun Matru Volcanic Field in Argentina (Inbar & Risso 2001). Slopes in the second group of cones (Cones 10–14, Table 1) are of the same order as slopes of the majority of the mounds analysed using high-resolution HiRISE imaging data which were interpreted as non-volcanic structures (Warner & Farmer 2008). Similarly, we identified these cones in the list of near-polar forms and observed the direct relationship between average slope and the morphometric parameter of surface-to-base ratio (Fig. 5). It should be noted that degradation of cinder cones through mass wasting and erosion provide different formation mechanism from pristine volcanic morphology. Therefore, the volcanic forms created by basaltic volcanism will be considerably different from the cinder cones of similar age. Following the Earth analogy, the cones with the morphometric parameters of slope ( $9^{\circ}$ – $12^{\circ}$ ) and surface-to-base ratio (1.09–1.15) might be associated with the volcanic activity as a result of small explosive eruptions. These values correspond well with the morphometric characteristics of older cinder cones in Kamchatka (2–10 Kyr) and Golan Heights ( $\sim 1$  Ma). However, the direct comparison of the morphometric parameters might not be appropriate due to DTM resolution that affects the morphometric parameters of cones in a way similar to that of erosion by reducing the topography and slope. In that case, young cinder cones depicted on a coarse resolution DTM can produce morphometric values similar to those of older cones calculated from DTM of higher resolution.

Assuming the volcanic origin of the studied Chasma Boreale mounds, Cones 1 and 2 (Table 1) can be considered the youngest cinder cones in the North Polar Region of Mars, with potential to be the youngest Martian permafrost. The terrestrial thermophilic psychrotolerant microbial inhabitants of the volcanic permafrost may suggest the hypothesis of existing microorganisms that may be found in permafrost around the young Martian cinder cones. Ongoing extension of HRSC DTM coverage over additional regions will contribute to better understand the volcanic history of the Martian North Polar Region.

Identification of the sites with a high possibility for microbial life existence is one of the most challenging issues in Mars exploration. The unique combination of the geological conditions that form young permafrost in volcanic cinder cones on Mars provides the environment that allowing for life preservation. Among the Martian geological assemblages, only volcanic permafrost is proximal to apply the terrestrial analogy of microbial thermophilic communities. In this perspective, morphometric analysis provides a way of selection of the younger volcanic cinder cones with higher potential for microbial life.

### Acknowledgements

This paper is dedicated to the memory of David Gilichinsky whose vision of the microbial life preservation in Martian permafrost has inspired the present work.



## References

- Abramov, A., Gruber, S. & Gilichinsky, D.A. (2008). Mountain permafrost on active volcanoes: field data and statistical mapping, Klyuchevskaya volcano group, Kamchatka, Russia. *Permafrost Periglacial Process.* **19**, 261–277.
- Berman, D.C. & Hartmann, W.K. (2002). Recent fluvial, volcanic, and tectonic activity on the Cerberus plains of Mars. *Icarus* **159**, 1–17.
- Bloomfield, K. (1975). A late-quaternary monogenetic volcanic field in central Mexico. *Geologischen Rundschau* **64**, 476–497.
- Broz, P. & Hauber, E. (2012). A unique volcanic field in Tharsis, Mars: pyroclastic cones as evidence for explosive eruptions. *Icarus* **218**, 88–99.
- Broz, P., Cadek, O., Hauber, E. & Rossi, A.P. (2014). Shape of scoria cones on Mars: insights from numerical modeling of ballistic pathways. *Earth Planet. Sci. Lett.* **406**, 14–23.
- Carr, M.H. (2006). *The Surface of Mars*. pp. 43–76. United States of America, Cambridge University Press, New York.
- Cousins, C.R. & Crawford, I.A. (2011). Volcano-ice interaction as a microbial habitat on earth and Mars. *Astrobiology* **11**, 695–710.
- Dohrenwend, J.C., Wells, S.G. & Turrin, B.D. (1986). Degradation of quaternary cinder cones in the Cima volcanic field, Mojave Desert, California. *Geol. Soc. Am. Bull.* **97**, 421–427.
- Dóniz, J., Romero, C., Coello, E., Guillén, C., Sánchez, N., García-Cacho, L. & García, A. (2008). Morphological and statistical characterization of recent mafic volcanism on Tenerife (Canary Islands, Spain). *J. Volcanol. Geotherm. Res.* **173**, 185–195.
- Fagents, S.A. & Wilson, L. (1996). Numerical modelling of ejecta dispersal from transient volcanic explosions on Mars. *Icarus* **123**, 284–295.
- Fishbaugh, K.E. & Head, J.W. (2002). Chasma Boreale, Mars: topographic characterization from Mars Orbiter Laser Altimeter data and implications for mechanisms of formation. *J. Geophys. Res.* **107**, 1–26.
- Flores, P.A., Amenábar, M.J. & Blamey, J.M. (2013). Hot environments from Antarctica: source of Thermophiles and Hyperthermophiles, with potential biotechnological applications. In *Thermophilic Microbes in Environmental and Industrial Biotechnology*, ed. Satyanarayana, T., Littlechild, J., Kawarabayasi, Yu., pp. 99–118. Springer, Netherlands.
- Garvin, J.B., Sakimoto, S.E.H., Frawley, J.J., Schnetzler, C.C. & Wright, H.M. (2000). Topographic evidence for geologically recent near-polar volcanism on Mars. *Icarus* **145**, 648–652.
- Gilichinsky, D.A. & Rivkina, E.M. (2011). Permafrost microbiology. In *Encyclopedia of Geobiology*, ed. Reitner, J., Thiel, V., pp. 726–732. Springer, Verlag.
- Gilichinsky, D. *et al.* (2007). Microbial populations in Antarctic permafrost: biodiversity, state, age, and implication for astrobiology. *Astrobiology* **7**, 275–311.
- Gilichinsky, M., Melnikov, D., Melekestsev, I., Zaretskaya, N. & Inbar, M. (2010). Morphometric measurements of cinder cones from digital elevation models of Tolbachik volcanic field in Central Kamchatka. *Can. J. Remote Sens.* **36**, 287–300.
- Gilichinsky, D., Rivkina, E., Vishnivetskaya, T., Gomez, F., Mironov, V., Lamey, J., Ramos, M., de Pablo, A., Castro, M. & Boehmwald, F. (2010). Habitability of Mars: Hyperthermophiles in Permafrost. In *38th COSPAR Scientific Assembly*, p. 11.
- Hasenaka, T. & Carmichael, I.S.E. (1985). A compilation of location, size, and geomorphological parameters of volcanoes of the Michoacan–Guanajuato volcanic field, central Mexico. *Geofis. Int.* **24**, 577–607.
- Herbold, C.W., Lee, C.K., McDonald, I.R. & Cary, S.C. (2014). Evidence of global-scale aeolian dispersal and endemism in isolated geothermal microbial communities of Antarctica. *Nat. Commun.* **5**, 3875.
- Herkenhoff, K. & Plaut, J. (2000). Surface ages and resurfacing rates of the polar layered deposits on Mars. *Icarus* **144**, 243–255.
- Hodges, C.A. & Moore, H.J. (1994). Atlas of volcanic landforms on Mars. *U.S. Geological Survey Professional Report*, pp. 183–184.
- Hooper, D.M. (1995). Computer-simulation models of scoria cone degradation in the Colima and Michoacan–Guanajuato volcanic fields, Mexico. *Geofis. Int.* **34**, 321–340.
- Inbar, M. & Risso, C. (2001). A morphological and morphometric analysis of a high density cinder cone volcanic field – Payun Matru, south-central Andes, Argentina. *Z. Geomorphol.* **45**, 321–343.
- Inbar, M., Gilichinsky, M., Melekestsev, I. & Melnikov, D. (2008). A Morphological and Morphometric Study of Cinder Cones in Kamchatka and Golan Heights. *Proceedings of the Israel Geological Society Annual Meeting*, Nazareth, Israel, p. 44.
- Inbar, M., Gilichinsky, M., Melekestsev, I., Melnikov, D. & Zaretskaya, N. (2011). Morphometric and morphological development of Holocene cinder cones: a field and remote sensing study in the Tolbachik volcanic field, Kamchatka. *J. Volcanol. Geotherm. Res.* **201**, 301–311.
- Inbar, M., Lugo Hubp, J. & Villers Ruiz, L. (1994). The geomorphological evolution of the Paricutin cone and lava flows, Mexico, 1943–1990. *Geomorphology*, **9**, 57–76.
- Lanz, J.K., Wagner, R., Wolf, U., Kröcher, J. & Neukum, G. (2010). Rift zone volcanism and associated cinder cone field in Utopia Planitia, Mars. *J. Geophys. Res.* **115**, 1–21.
- Martin del Pozzo, A.L. (1982). Monogenetic vulcanism in Sierra Chichinautzin, Mexico. *Bull. Volcanol.* **45**, 9–24.
- Mironov, V., Shcherbakova, V., Rivkina, E. & Gilichinsky, D. (2013). Thermophilic bacteria *Geobacillus* genus from volcanic permafrost sediments. *Microbiology* **82**(3), 389–392.
- Mouginis-Mark, P.J., Wilson, L. & Zuber, M.T. (1992). The physical volcanology of Mars in *Mars*, ed. Kieffer, H.H., Jakosky, B.M., Snyder, C.W. & Matthews, M.S., pp. 424–452. University of Arizona Press, Tucson, AZ.
- Nemeth, K. (2011). From maars to scoria cones: the enigma of monogenetic volcanic fields. *Journal of Volcanology and Geothermal Research*, **201**, 1–4.
- Neukum, G. & van Gasselt, S. (2006). Recent volcanism at the Martian north pole. *Geophys. Res. Abstr.* **8**, 11103.
- Neukum, G., Jaumann, R., Hoffmann, H., Hauber, E., Head, J.W., Basilevsky, A.T., Ivanov, B.A., Werner, S.C., Van Gasselt, S. & Murray, J.B. (2004). Recent and episodic volcanic and glacial activity on Mars revealed by the high resolution stereo camera. *Nature* **432**, 971–979.
- de Pablo, M.A. & Komatsu, G. (2009). Possible pingo fields in the Utopia basin, Mars: Geological and climatic implications. *Icarus*, **199**, 49–74.
- Parfitt, E.A. & Wilson, L. (2008). *Fundamentals of Physical Volcanology*. Blackwell, Oxford, UK.
- Parrot, J.F. (2007). Three-dimensional parameterization: an automated treatment to study the evolution of volcanic cones. *Geomorphologie* **3**, 247–258.
- Pondrelli, M., Rossi, A.P., Ori, G.G., van Gasselt, S., Praeg, D. & Ceramicola, S. (2011). Mud volcanoes in Mars Geologic Record: the case of Firsoff Crater. *Earth and Planetary Science Letters*, **304**, 511–519.
- Porter, S.C. (1972). Distribution, morphology and size frequency of cinder cones on Mauna Kea volcano, Hawaii. *Geol. Soc. Am. Bull.* **83**, 3607–3612.
- Scott, D.H. & Trask, N.J. (1971). Geology of the Luna Crater volcanic field, Nye County, Nevada. *USGS Professional Paper*, 599-I, p. 22.
- Segerstrom, K. (1950). Erosion studies at Paricutin, State of Michoacán, Mexico. *U.S. Geological Survey Bulletin*, **965-A**, 1–164.
- Settle, M. (1979). The structure and emplacement of cinder cone fields. *Am. J. Sci.* **279**, 1089–1107.
- Warner, N.H. & Farmer, J.D. (2008). The origin of conical mounds at the mouth of Chasma Boreale. *J. Geophys. Res.* **113**, 1–28.
- Wilson, L. & Head, J.W. (1994). Mars: review and analysis of volcanic eruption theory and relationships to observed landforms. *Rev. Geophys.* **32**, 221–264.
- Wolfe, E.W., Ulrich, G.E. & Newhall, C.G. (1987). Geologic Map of the Northwest Part of the San Francisco Volcanic Field, North-central Arizona. USGS Misc. Field Stud. Map, MF1957.
- Wood, C.A. (1979). Monogenetic volcanoes of the terrestrial planets. In *10th, Lunar and Planetary Science Conf., Proc.*, Houston, Texas, 19–23 March, 1979 pp. 2815–2840. Pergamon Press, New York.
- Wood, C.A. (1980). Morphometric analysis of cinder cone degradation. *J. Volcanol. Geotherm. Res.* **8**, 137–160.